Generation of miR-141/200c conditional knockout mice from knockout-first, reporter-tagged parent and functional validation of the floxed allele

Sanjeev Kumar Yadav[1#], Rashmi Srivastava[1#], Mary-Katherine Cormier[1], Katie Lowther[2], Siu-Pok Yee[2,*], and Rajkumar Verma[1,*]

[1]Department of Neurosciences, UConn Health Farmington CT 06030

[2]Center for Mouse Genome Modification, UConn Health, Farmington CT 06030

[#]equal contribution

*Corresponding author

Rajkumar Verma

Assistant professor

Email: raverma@uchc.edu

ORCID ID: https://orcid.org/0000-0002-1123-6508

Sui-Pok Yee

Associate Professor

Email: syee@uchc.edu

ORCID: https://orcid.org/0000-0002-2427-401X

ABSTRACT

MicroRNAs (miRNAs) of the miR-200 family specifically miR-141 and miR-200c regulate neurogenesis, differentiation, and epithelial mesenchymal transitions in development. Dysregulation of these miRNAs is associated with several diseases including cancer and stroke. The Mirc13tm1Mtm/Mmjax mouse line, which targets the miR-141/200c cluster, was originally generated and described by Park et al. 2012 as a knockout-first, reporter-tagged insertion with conditional potential (conditional-ready) mouse line. To harness the full potential of this mouse line, it would require a two-step breeding process: breed with FLP mice to excise lacZ/neo cassettes followed by breeding with Cre to delete the floxed miRNA cluster(Park, et al. 2012). However, many studies either bypassed removal of the lacZ/Neo cassettes and treated the mouse line as Mirc13 knockouts or bred directly with Cre mouse lines, which could lead to unpredictable recombination and genotypes. In this study, we show that the presence of the Neo cassette influences expression of neighboring genes. We demonstrate that it is essential to follow the two-step breeding plan.

KEYWORDS: miR-141/200c cluster, lacZ/neo cassettes, Mirc13, microRNA, FLPo deleter

INTRODUCTION

microRNAs (miRNAs) are small, noncoding RNAs (~22 nucleotides) that regulate gene expression post-transcriptionally and play pivotal roles in development and disease. Originally discovered in C. elegans(Lee, et al. 1993; Wightman, et al. 1993) and later shown to be evolutionarily conserved across species(Pasquinelli, et al. 2000), miRNAs are now recognized as critical regulators in cardiovascular(Small, et al. 2010; van Rooij and Kauppinen 2014), neurological(Wu, et al. 2016; Verma, et al. 2018), and oncogenic pathways(Humphries and Yang 2015; Jin, et al. 2017), holding significant potential for therapeutic applications(Janssen, et al. 2013; Verma, et al. 2018) While cell-based studies have elucidated many of these mechanisms, in vivo models remain essential to fully understand the functions of miRNAs under physiological and pathological contexts.

Park et al. established a key genetic resource for in vivo miRNA investigation by generating conditional knockout-first mouse lines for conserved miRNAs, including the miR-141/200c cluster (Mirc13tm1Mtm/Mmjax)(Park, et al. 2012). This cluster, located on mouse chromosome 6, encodes two members of the miR-200 family implicated in neurogenesis(Choi, et al. 2008; Beclin, et al. 2016), differentiation(Zhang, et al. 2015), epithelial–mesenchymal transition(Tseng, et al. 2017), cancer(Chen, et al. 2013; Jin, et al. 2017), stroke(Small, et al. 2010; Yadav, et al. 2024), and Alzheimer's disease(Wu, et al. 2016). To make miR-141/200c cluster KO mice, Park et al. used a targeting vector to incorporate a lacZ reporter and β-actin-neo selection cassette flanked by FRT sites and loxP sites surrounding the miR-141/200c cluster. This enabled a two-step recombination strategy: first, FLP-mediated removal of the lacZ/neo cassette generates a clean conditional (floxed) allele, and then Cre-mediated excision removes the miR-141/200c cluster(Park, et al. 2012). However, many subsequent studies bypassed the essential FLP recombination step(Guan, et al. 2018; Hoefert, et al. 2018; Ji, et al. 2018; Liu, et al.

76 2018; Wu, et al. 2019; Xu, et al. 2025). In such cases, the lacZ/neo selection cassette
77 remains in the targeted allele, which can transcriptionally silence neighboring
78 genes(Testa, et al. 2004; Raja, et al. 2024) or alter local expression patterns due to the
79 strong β-actin promoter driving the cassette(Pham, et al. 1996), thereby confounding
80 phenotypic interpretation. Other studies attempted cassette removal using FLPe deleter
81 strains; however, several commonly used FLPe lines exhibit variable recombination
82 efficiency, which may lead to incomplete or mosaic excision depending on the deleter
83 strain and genomic target locus(Tran, et al. 2017; Mostofa, et al. 2022; Tran, et al. 2024).
84 Consequently, a small proportion of animals may retain the selection cassette despite
85 FLPe breeding, resulting in heterogeneous genotypes within experimental cohorts.
86 Several studies have reported that residual selection cassettes can unintentionally
87 suppress the expression of nearby genes(Olson, et al. 1996; Pham, et al. 1996; Skarnes,
88 et al. 2011). In the case of the miR-141/200c cluster, genes located in close proximity—
89 including *Ptpn6, Phb2, Atn1, Eno2,* and *Eng1* (www.Ensembl.org)—may be affected.
90 Because these genes are known to play important roles in neuronal function and
91 mitochondrial integrity(Whitton, et al. 1993; Bernabeu, et al. 2009; Xu, et al. 2014; Isgrò,
92 et al. 2015; He, et al. 2023), unintended suppression could lead to misleading
93 interpretations or the apparent loss of phenotype in knockout mice generated without prior
94 removal of the neo cassette.

95 To overcome these limitations, we optimized the original “knockout-first” design
96 suggested by Park et al. 2012(Park, et al. 2012) by employing high-efficiency FLPo
97 deleter mice instead of FLPe or β-actin-FLP strains(Raymond and Soriano 2007; Wu, et
98 al. 2009; Kranz, et al. 2010). FLPo recombinase exhibits greater thermostability and
99 recombination efficiency in mammalian cells(Raymond and Soriano 2007; Wu, et al.
100 2009; Kranz, et al. 2010), ensuring complete excision of the lacZ/neo cassette and

101 restoration of an unperturbed floxed allele before Cre-mediated deletion. This refinement
102 minimizes off-target silencing, preserves adjacent gene expression, and produces
103 genetically clean global or tissue-specific miR-141/200c knockouts. Here, we present a
104 validated, optimized, and detailed breeding strategy using FLPo deleter mice that ensures
105 complete removal of the lacZ/neo cassette and precise deletion of the miR-141/200c
106 cluster. This work establishes a robust framework for generating unambiguous cell-
107 specific or conditional knockouts of the miR-141/200c cluster, facilitating accurate studies
108 of miRNA function in neural and systemic disease models.
109

110 **MATERIAL AND METHODS**

111 ***Mouse Strains***

112 All mouse strains used in this study were obtained from the Jackson Laboratory (Bar
113 Harbor, ME): Mirc13^{tm1Mtm}/Mmjax line (MMRRC stock #34657(Park, et
114 al. 2012)) (hereon referred as *Mirc13*^{tm1} line); B6.129S4-
115 Gt(ROSA)26Sor^{tFLP})Sor/J (ROSA-FLPo; Jax# 012930)(Raymond and
116 Soriano 2007); 129S1/Sv-Hprt1^{tm1(CAG-cre)Mnn}/J) (Hprt-Cre; Jax#
117 004302)(Tang, et al. 2002) and B6.129P2-Lyz2^{tm1(cre)Ifo}/J) (LysMCre;
118 Jax # 004781)(Clausen, et al. 1999). All mice were maintained under standard
119 conditions at ambient temperature and humidity, with ad libitum access to pellet food
120 and water. All animal studies were approved by the Institutional Animal Care and Use
121 Committee at the University of Connecticut Health Center.

122 ***Genotyping of Mouse Strains***

123 Tail biopsies (~4 mm) were collected in DNase-free microtubes and incubated in 50 ml of
124 alkali buffer (25mM NaOH and 0.2mM EDTA) at 100°C for one hour and an equal volume
125 of neutralization buffer (40mM Tris buffer, pH 7.5) was added. One microliter of the DNA

126 was used for PCR genotyping with 2× JumpStart™ Taq ReadyMix (Sigma-Aldrich
127 P2893). Primer pairs are listed in Table 1. PCR was performed according to the
128 manufacturer's instructions. PCR products were fractionated on 2% agarose gels
129 prepared in 1× Tris-Acetate-EDTA (TAE) buffer (Bio-Rad 1610743) with SYBR™ Safe
130 DNA stain (Invitrogen S33102) and visualized under UV illumination.

131 ***β-Galactosidase (lacZ) Staining***

132 A β-galactosidase staining kit (Sigma-Aldrich GALS-1KT) was used to assess lacZ
133 reporter expression. Mice were deeply anesthetized with Avertin (250 mg/kg, i.p.),
134 perfused with ice-cold PBS, and brains were collected for cryosections (10 µm, Superfrost
135 Plus slides). Sections were fixed with fixation solution (provided with kit) for 10 min, and
136 LacZ expression was determined using a β-galactosidase staining kit according to
137 manufacturer's instructions. Slides were mounted in 70% glycerol and imaged under
138 bright-field microscopy.

139 ***RNA Isolation, cDNA Synthesis, and Real-Time PCR***

140 Total RNA was extracted from the olfactory bulb, frontal and parietal cortex,
141 hippocampus, cerebellum, heart, lung, and liver using TRIzol or miRVana kits (Ambion
142 Life Technologies, 15596018, AM1560). cDNA synthesis for miRNAs and mRNAs was
143 performed using the TaqMan MicroRNA Reverse Transcription Kit (Thermo Fisher
144 4366596) and iScript cDNA Synthesis Kit (Bio-Rad 1708891), respectively. TaqMan
145 assays included miR-141-3p (000463), miR-200c-3p (002300), U6snRNA (001973),
146 *Ptpn6* (Mm00469153_m1), *Phb2* (Mm00476104_m1), *Atn1* (Mm00492256_m1), *Eno2*
147 (Mm00469062_m1), *Emg1* (Mm00496596_m1), and *Gapdh* (Mm99999915_g1) (Thermo
148 Fisher Scientific). PCR was performed using TaqMan Universal PCR Master Mix II (No
149 UNG; Thermo Fisher 4440040). Relative expression was determined by the 2^–ΔΔCt
150 method using U6 and Gapdh as normalizers for miRNA and mRNA targets, respectively.

151 ***RNA Fluorescence In Situ Hybridization (RNA-FISH)***

152 RNA-FISH was performed using Molecular Instruments protocols. Fixed tissue sections
153 were pre-hybridized at 37 °C and incubated overnight with 16 nM of the miR-141-3p
154 probe. Following stringent SSCT washes, signal amplification was performed using snap-
155 cooled hairpins (h1/h2; 6 pmol each) incubated overnight at room temperature. Sections
156 were mounted with antifade DAPI UltraCruz Mounting Solution (Santa Cruz SC-24941)
157 and imaged by fluorescence microscopy.

158 ***Statistical Analysis***

159 Data are presented as mean ± SD. Relative expression values derived from the 2^–ΔΔCt
160 method were used for statistical analysis. Statistical analyses were performed using
161 GraphPad Prism (San Diego, CA). Comparisons between two groups were conducted
162 using a two-tailed unpaired Student's *t*-test, while multiple group comparisons were
163 analyzed using one-way ANOVA followed by Bonferroni post hoc correction. Data
164 distribution was assessed for normality prior to applying parametric tests. A p value < 0.05
165 was considered statistically significant. Blinding was implemented during data acquisition
166 and analysis where feasible. Each dot In graphs represent an individual mouse.

167

168

169

170

171

172

173

174

175

176

177

178

Target	Primer (F/R)	Primer Sequence (5'-3')	Amplicon size (bp)
Mirc13	Jax 11311 (F)	CAACAGCCTCTGACCTTTAACC	340 (WT)
	Jax 11312 (R)	CCTTCTGGGCAGACAAGAATAC	432 (floxed)
Mirc13	mir5Fn3 (F)	CCGGCAGGTGAAGGAGGAAG	1315 (WT)
	Jax 11312 (R)	CCTTCTGGGCAGACAAGAATAC	352 (KO)
lacZ	oIMR3054 (lacZ F)	ATCCTCTGCATGGTCAGGTC	315
	oIMR0040 (LacZ R)	CGTGGCCTGATTCATTCC	
neo	oIMR6916 (Neo F)	CTTGGGTGGAGAGGCTATTC	280
	oIMR6917 (Neo R)	AGGTGAGATGACAGGAGATC	
Flpo	oIMR8545 (F)	AAAGTCGCTCTGAGTTGTTAT	300
	oIMR8052 (R)	GCGAAGAGTTTGTCCTCAACC	
Rosa26	oIMR8545 (F)	AAAGTCGCTCTGAGTTGTTAT	603
	oIMR8546 (R)	GGAGCGGGAGAAATGGATATG	
Cre	oIMR1084 (F)	GCGGTCTGGCAGTAAAAACTA TC	100
	oIMR1085 (R)	GTCAAACAGCATTGCTGTCAC TT	

179

180 **Table1**. List of different sets of primer sequences (with amplicon size) used in PCR

181 amplification

182

183

184 **RESULTS**

185 ***Genomic Organization of the Mirc13 Mouse Lines and Genotyping of the Mouse***
186 ***Lines***

187 The Mirc13^{tm1Mtm}/Mmjax line (MMRRC stock #34657) mouse line,
188 hereon referred as Mirc13^{tm1} line, available from the Jax MMRCC is a knockout-first,
189 reporter-tagged insertion with conditional potential (conditional-ready) mouse line. The
190 miR-141/200c (Mirc13) cluster is located within intron 1 of the lncRNA, *GM15884*. As
191 shown in Fig 1A, the targeted allele contains an *engrailed 2* (En2) splice acceptor followed
192 by an internal ribosomal entry site (ires) sequence coupled to lacZ reporter sequence and
193 polyadenylation signal sequence. This mouse line was originally generated by gene
194 targeting in embryonic stem (ES) cells via homologous recombination. A β-actin-Neo
195 cassette was placed 3' of the lacZ polyA sequence in the targeting vector to confer G418
196 selection to help screen for targeted ES cell clones. The Neo cassette and the lacZ
197 reporter was separated by a single loxP site. The lacZ/Neo sequences were flanked by a
198 pair of Frt sites and inserted into intron 1 of *GM15884* 5' of the floxed *Mirc13* cluster. With
199 the polyadenylation sequence placed 3' of the lacZ sequence, it will terminate any
200 *GM15884* 3'-downstream transcription, including the Mirc13 cluster, therefore, this mouse
201 line is a double knockout of both *GM15884* and *Mirc13* cluster (knockout first). We first
202 performed PCR genotyping of Mirc13$^{tm1/+}$ pups using primer pairs as shown in Table 1.
203 As shown in Fig 2A, we detected amplicon of 340 bp and 432 bp specific to the Mirc13
204 WT and floxed allele, respectively. We were also able to amplify fragments of 315 bp and
205 280 bp specific to lacZ and Neo, respectively, confirming the genotype of the Mirc13$^{tm1/+}$
206 mice we obtained from MMRCC/Jax. We then bred the Mirc13$^{tm1/+}$ pups together to obtain
207 Mirc13$^{tm1/tm1}$ pups for expression analyses as described below. PCR genotyping only
208 detected the 432 bp fragment specific to the Mirc13 floxed allele as well as the lacZ and

209 neo specific amplicons. The absence of the Mirc13 WT specific amplicon of 340 bp

210 confirmed WT that these were homozygous Mirc13^{tm1} mice (Fig 2A).

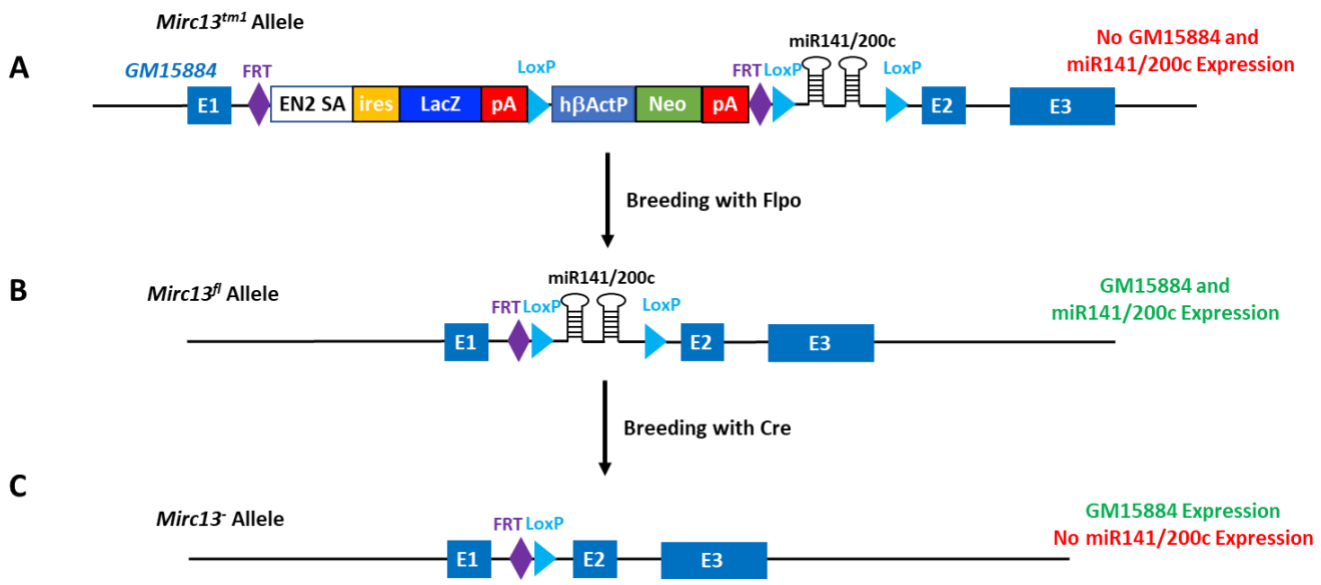

211 **Fig. 1** Genomic organization of Mirc13tm1 allele and after Flpo and Cre mediated

212 recombination. **A** The Mirc13tm1 mouse line was originally designed as a a knockout

213 first, reporter-tagged insertion with conditional potential (conditional-ready) mouse line

214 for Mirc13 (miR-141/200c cluster). Insertion of the en-lacZ gene trap cassette with

215 prevent any subsequent 3'-downstream transcription leading to the lack of GM15884

216 and Mirc13 expression. **B** When these mice were bred with Rosa26-Flpo, Flpo will

217 facilitate excision of the LacZ/Neo cassette to generate the Mirc13fl allele with wildtype

218 level of expression of both GM15884 and mir141/200c. **C** When Mirc13fl mice were

219 bred with Cre, Cre will mediate excision of the Mirc13 cluster sequence to generate

220 Mirc13- allele with wildtype GM15884 expression and the lack of miR141/200c

221 expression.

222

223 As described above, the lacZ/Neo sequences are flanked by a pair of Frt sites,

224 which can be excised by Flp recombinase resulting in the generation of functional *Mirc13*

225 conditional knockout (conditional later) mice expressing both *GM15884* and miR-
226 141/200c as shown in Fig 1B. To accomplish this, we bred Mirc13$^{tm1/+}$ mice with
227 Rosa26$^{Flpo/+}$ mice (Jax #012930). As shown in Fig 2B, genotyping results showed the
228 absence of lacZ specific amplicon of 315 bp (lane 1 and 2) thereby confirming successful
229 excision of the lacZ/Neo cassette and generation of Mirc13$^{fl/+}$ pups. To generate Mirc13
230 knockout (KO) mice, we bred Mirc13$^{fl/+}$ pups with Hprt$^{CAG\text{-}Cre/+}$ mice (Fig1C). To detect the
231 knockout allele, a forward primer (mir5Fn3) was designed to target the region upstream
232 of the frt/loxP site and was paired with the Jax 11312 reverse primer downstream of the
233 3' loxP site. This primer pair will generate two amplicons, one specific to the WT allele
234 (1.3 kb) and one specific to the knockout allele that is smaller in size due to Cre-mediated
235 recombination (353 bp). As shown in Fig 2C, PCR genotyping showed that we were able
236 to amplify the predicted fragments of 1.3 kb (lane 1) or 352 bp (lanes 2 and 3) specific to
237 Mirc13 WT and KO alleles, respectively. We anticipated that we should obtain either
238 Mirc13$^{+/+}$ or Mirc13$^{+/-}$ pups from this breeding pair. However, we did not detect both
239 amplicons in heterozygous Mirc13$^{+/-}$ mice. This is most likely because our PCR conditions
240 favors amplification of the smaller amplicon specific to the knockout allele, and the pups
241 shown in Fig 2C lanes 2 and 3, were Mirc13$^{+/-}$ mice. We further bred Mirc13$^{+/-}$ mice
242 together and mice were genotyped using the same primers described above for the
243 knockout allele and also with the original Jax primer pairs specific to the 3' loxP site in
244 order to detect the presence or absence of the WT allele. We were able to obtain Mirc13^{-}
245 $^{/-}$ mice as shown by PCR genotyping that was positive only for the KO-specific amplicon
246 and no WT-specific amplicon was observed (Fig 2D, lane 2). The other littermates were

247 either Mirc13$^{+/-}$, which were positive for both amplicons (Fig 2D lanes 1 and 4) or Mirc13$^{+/+}$

248 as revealed by the presence of the WT-specific amplicon only (Fig 2D lane 3).

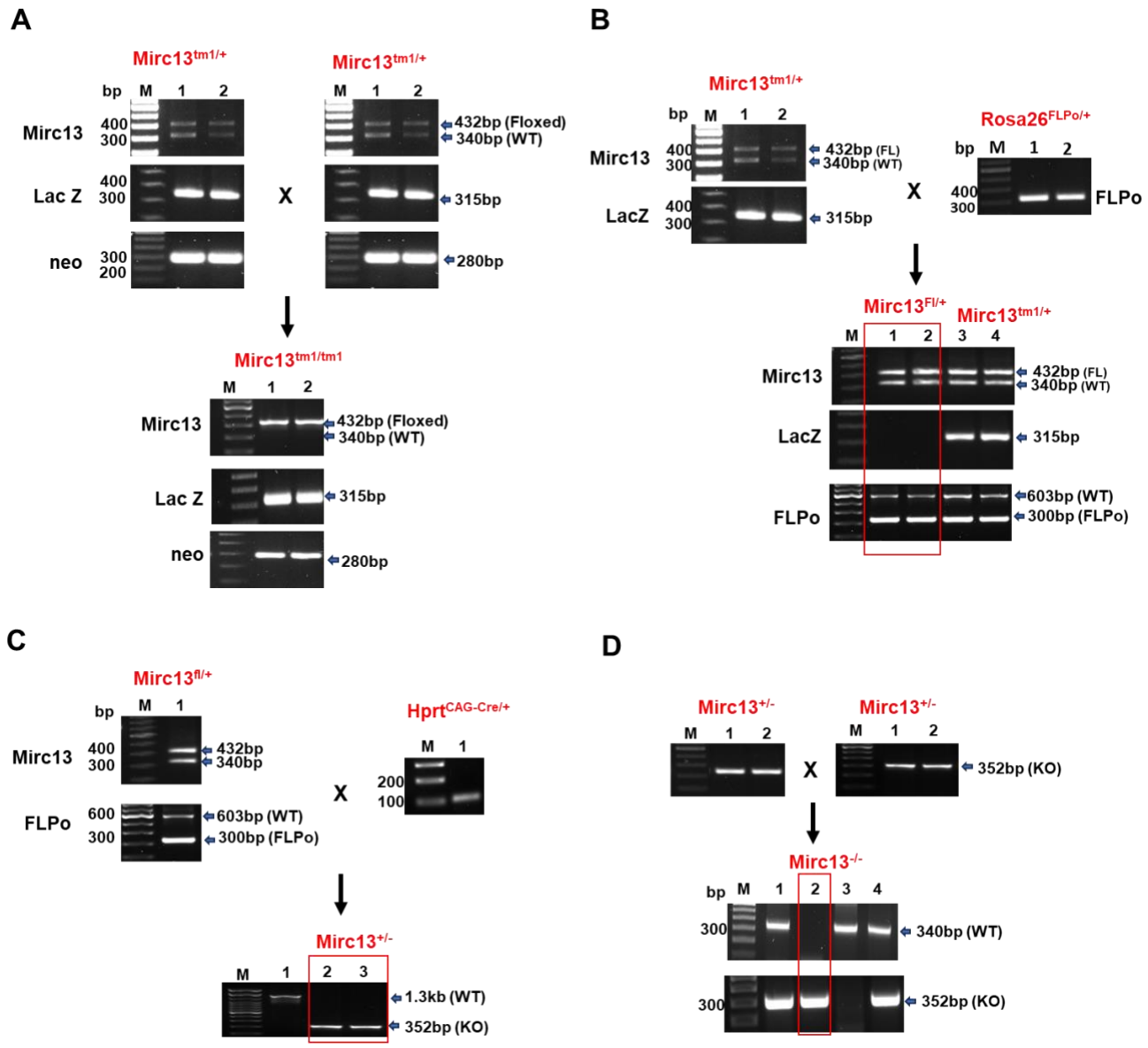

249 **Fig. 2** PCR Genotyping of mice with different *Mirc13* alleles. **A** Generation of *Mirc13$^{tm1/tm1}$*

250 mice by breeding *Mirc13$^{tm1/+}$* mice, which contain lacZ/Neo cassette and floxed *Mirc13*

251 *sequence*, together; **B** Removal of lacZ and Neo cassette by breeding *Mirc13$^{tm1/+}$* mice

252 with *Rosa26$^{FLPo/+}$* mice. Positive *Mirc13$^{fl/+}$* mice, lacking the lacZ/Neo cassette (315 bp

253 amplicon), were marked by a red box; **C** Generation of heterozygous *Mirc13$^{+/-}$* (KO) mice

254 by breeding *Mirc13$^{fl/fl}$* with *Hprt$^{CAG-Cre/+}$* mice. Positive *Mirc13$^{+/-}$* mice, lacking a 432 bp

255 amplicon specific to the *Mirc1fl*$^{1/+}$ allele, were marked by a red box; **D** Heterozygous
256 *Mirc13*$^{+/-}$ mice were bred together to generate homozygous *Mirc13*$^{-/-}$ global homozygous
257 KO mice. These mice were identified by the presence of a KO-specific amplicon (352 bp)
258 and the loss of wt specific amplicon (340 bp) and were marked by the red box. PCR were
259 performed using primer pairs as shown in Table 1 and amplicons specific for lacZ is 315
260 bp, *Mirc*$^{+}$ is 340 bp, *Mirc13*^{fl} is 432 bp, *Mirc13*$^{-}$ is 352 bp, Rosa26 is 603 bp, Flpo is 300
261 bp and Cre is 100 bp.

262 ***Expression Analysis of Homozygous Mirc13^{tm1} Mice***

263 The En2 splice acceptor is designed to facilitate splicing between exon 1 of
264 *GM15884* with the ires-lacZ reporter sequence. Thus, the targeted allele will generate a
265 fusion transcript consisting of exon 1 of the disrupted endogenous *GM15884*, a lncRNA,
266 ires and lacZ coding sequence. PCR genotyping confirmed presence of the lacZ reporter
267 (Fig 2A). Since the ires-lacZ gene trap cassette is inserted into intron 1 of the endogenous
268 *GM15884* and placed under the *GM15884* transcriptional regulatory sequence, lacZ
269 expression will faithfully recapitulate spatiotemporal expression of the endogenous
270 *GM15884* LncRNA, which should also reveal the spatiotemporal expression of the miR-
271 141/200c cluster (Mirc13) located within intron 1 of *GM15884*. However, the
272 polyadenylation sequence placed 3' with respect to the lacZ sequence will prevent further
273 3'-downstream transcription, including the Mirc13 cluster, to accomplish the knockout first
274 task. This mouse line is practically a double knockout of both *GM15884* and Mirc13
275 cluster.

276 We first examined lacZ expression, which should reveal endogenous expression of
277 GM15884 and miR-141-3p and miR-200c-3p, by x-gal staining of b-galactosidase, the
278 gene product of lacZ. Strong b-galactosidase activity was detected in the olfactory bulb,
279 with weaker staining near the lung–tracheal junction, and minimal expression in the heart

280 and liver (Fig. 3A). To further characterize expression of Mirc13, we isolated total RNA
281 from the brain olfactory bulb and lungs of Mirc13$^{tm1/tm1}$ and Mirc13$^{+/+}$ mice and performed
282 RT-qPCR to examine the level of miR-141-3p and miR-200c-3p expression. Our results
283 showed that miR-141-3p and miR-200c-3p were highly expressed in the olfactory bulb
284 and lung (ΔCT < 5), whereas heart and liver exhibited lower expression levels (ΔCT > 10)
285 in Mirc13$^{+/+}$ mice, consistent with the miRNA expression atlas(Rishik, et al. 2025) (Fig.
286 3B and C). A significant and near-complete reduction of miR-141-3p (Fig 3D &E and
287 miR-200c-3p (Fig. 3F & G) expression was observed in the olfactory bulb and lungs in
288 Mirc13$^{tm1/tm1}$ mice. Data are presented as mean ± SD (*p < 0.05 vs. WT control).

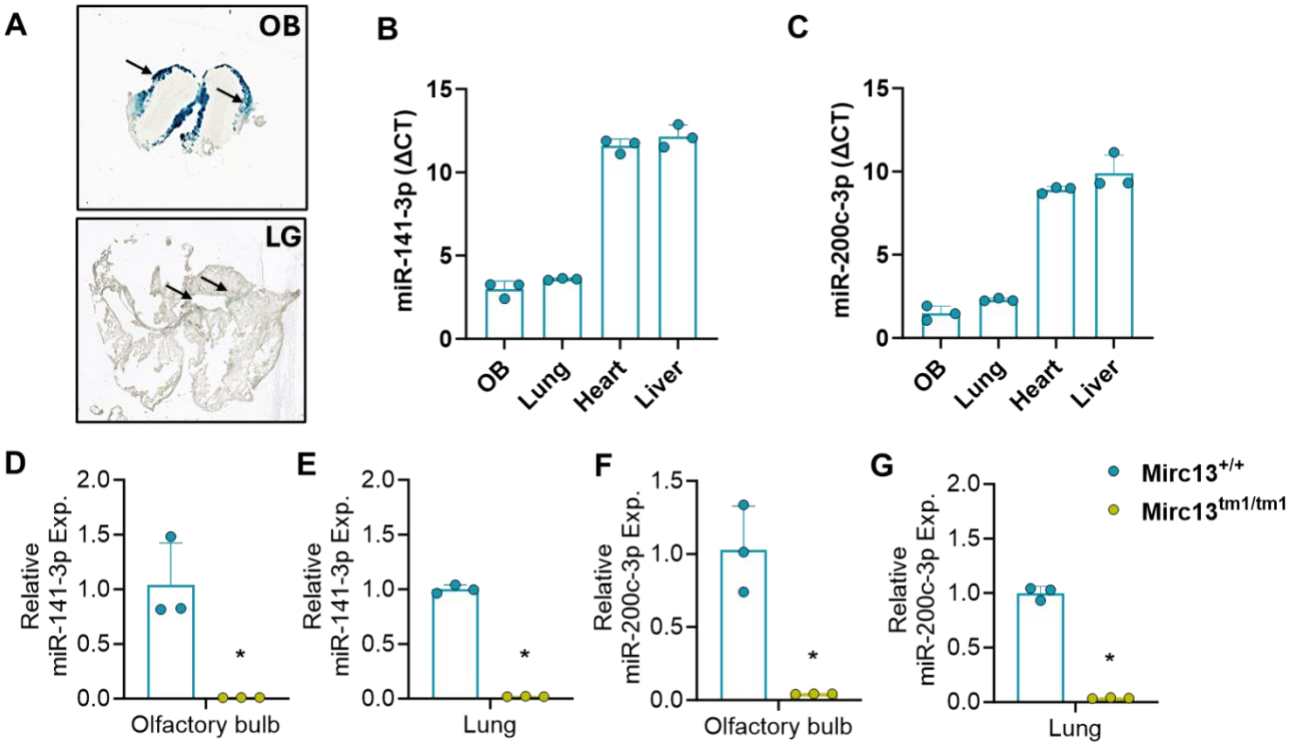

289

290 **Fig. 3** Expression analyses of *Mirc13$^{tm1/tm1}$* mice. **A**. LacZ expression as revealed by x–
291 gal staining of olfactory bulb (OB) and lung (LG); **B**, **C** Basal expression of miR-141-3p
292 and miR-200c-3p was analyzed by RT-qPCR in olfactory bulb, lung, heart and liver of
293 wildtype mice. Relative expressions of miR-141-3p (**D &E**) and miR-200c-3p (**F & G**)
294 were assessed by RT-qPCR in the brain olfactory bulb and lungs of Mirc13$^{tm1/tm1}$ KO mice
295 compared to (Mirc13$^{+/+}$) littermate control mice. Data are presented as mean ± SD (*p <

296 0.05 vs. Mirc13$^{+/+}$ littermate control). Blue column denotes Mirc13$^{+/+}$ and yellow column
297 denotes Mirc13$^{tm1/tm1}$.

298 ***Presence of β-actin-Neo cassette leads to Transcriptional Interference of***
299 ***Neighboring Genes***

300 The Mirc13^{tm1} mouse line was originally generated by gene targeting in
301 embryonic stem cells via homologous recombination. A lacZ polyA sequence was
302 included in the targeting vector to confer G418 positive selection to screen for targeted
303 ES cell clones. However, the Neo cassette containing a strong ubiquitous β-actin
304 promoter was not removed prior to generation of the Mirc13^{tm1} mouse line. It has been
305 reported that insertion of a strong promoter within a gene would not only disrupt
306 endogenous expression, but it could also potentially lead to dysregulation of
307 neighboring genes and resulted in unanticipated phenotypic alterations(Olson, et al.
308 1996; Pham, et al. 1996; Skarnes, et al. 2011).

309 To further investigate the influence of the b-actin-Neo cassette on neighboring
310 gene expression, we identified 5 genes, Ptpn6, Phb2, Atn1, Eno2 and Emg1 that are
311 important for brain function, located within 50 kb from Mirc13. Total RNA was isolated
312 from olfactory bulb of Mirc13$^{+/+}$ and Mirc13$^{tm1/tm1}$ mice and the levels of neighboring gene
313 expression were characterized by RT-qPCR. As shown in Fig 4A-C , expression of Ptpn6,
314 Phb2, and Atn1 was significantly decreased (±>1.5 folds threshold, $p<0.05$) in
315 Mirc13$^{tm1/tm1}$ mice as compared to Mirc13$^{+/+}$ mice, while Eno2 and Emg1 showed a similar
316 decreasing trend (Fig 4D and E). In Mirc13$^{-/-}$ mice, the expression Ptpn6, Phb2, Atn1,
317 Eno2, and Emg1 did not show significantly change (±>1.5 folds threshold, $p<0.05$) as
318 compared to Mirc13$^{fl/fl}$ mice (Fig 4F to J). Our results showed that the presence of b-actin-
319 Neo cassette within GM15884 affects neighboring gene expression and it is therefore

320 essential to excise the cassette prior to obtaining transparent and interpretable
321 subsequent data.

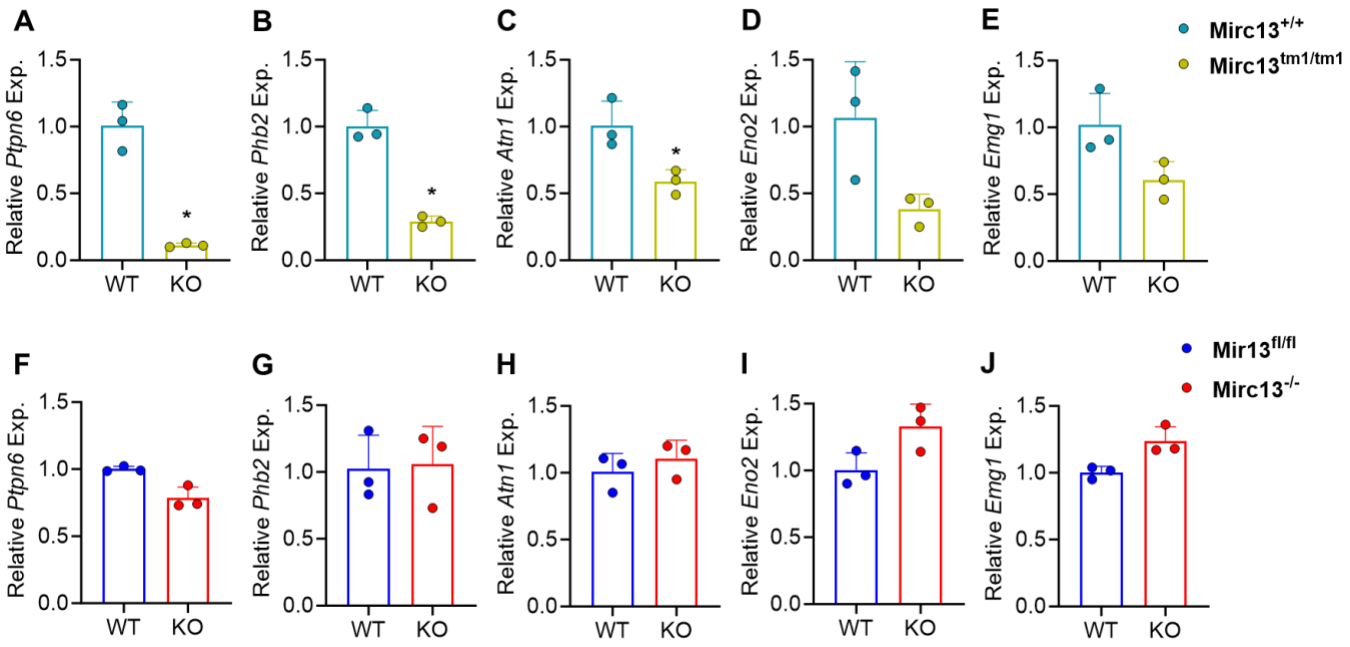

322 **Fig. 4** Expression analysis of Mirc13 neighboring genes. Total RNA was isolated from
323 olfactory bulb (OB) of Mirc13$^{tm1/tm1}$ and Mirc13$^{-/-}$ mice and corresponding negative
324 littermate (Mirc13$^{+/+}$ and Mirc13$^{fl/fl}$). Expression of Ptpn6 (**A** and **F**), Phb2 (**B** and **G**), Atn1
325 (**C** and **H**), Eno2 (**D** and **I**), and Emg1 (**E** and **J**) were assessed by RT-qPCR. Data are
326 presented as mean ± SD (*$p < 0.05$ vs. Mirc13$^{+/+}$ control. Light blue column denotes RNA
327 obtained from Mirc13$^{+/+}$; Yellow column denotes RNA obtained from Mirc13$^{tm1/tm1}$; dark
328 blue column denotes RNA from Mirc13$^{fl/fl}$ and red column denotes RNA isolated from
329 Mirc13$^{-/-}$ mice.

330 ***Expression Analysis of miR-141-3p and miR-200c-3p in Mirc13$^{-/-}$ mice***

331 We further characterized expression of miR-141-3p and miR-200c-3p in Mirc13$^{-/-}$
332 and their corresponding Mirc13$^{fl/fl}$ mice in the brain. We isolated total RNA from different
333 regions of the brain, including olfactory bulb (OB), frontal cortex (FC), parietal cortex (PC),
334 hippocampus (HP), and cerebellum (CB), from mice of both genotypes. Our results

335 showed both miR-141-3p and miR-200c-3p were highly expressed in the OB (ΔCT < 5; it
336 is to be noted that lower ΔCT indicate higher expression), while their expression in other
337 regions was very low (ΔCT > 10) (Fig 5A and B). Notably, the OB of Mirc13$^{-/-}$ mice showed
338 no detectable expression of miR-141-3p by RNA-FISH (Fig 5C). This finding was further
339 confirmed by RT-qPCR, which demonstrated a marked reduction of both miRNAs (miR-
340 141-3p & miR-200c-3p) in the OB almost negligible (Fig 5D and I), along with significantly
341 decreased expression in the FC (Fig 5E and J), PC (Fig 5F and K), HP (Fig 5G and L),
342 and CB (Fig 5H and M) of Mirc13$^{-/-}$ mice as compared to Mirc13$^{fl/fl}$ mice.

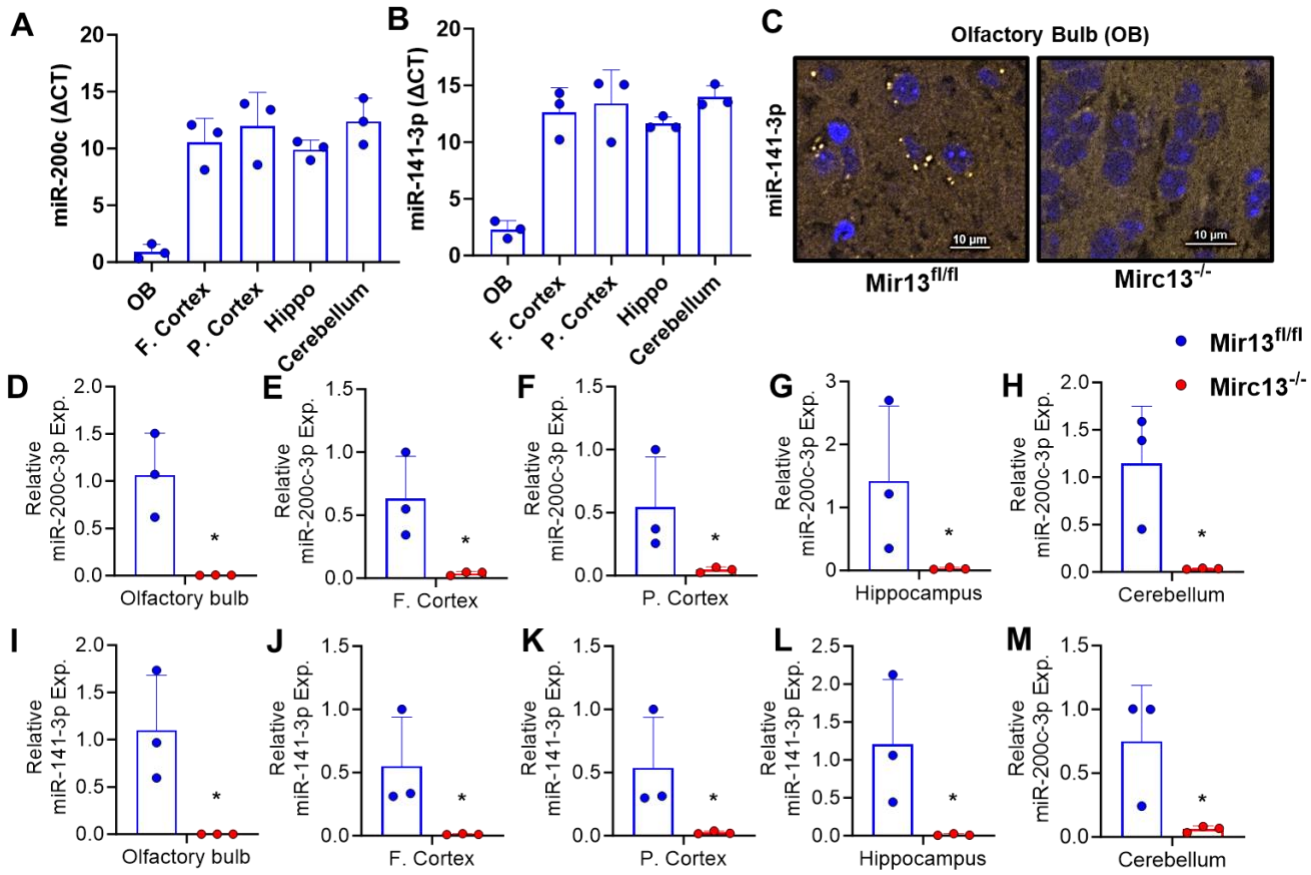

343 **Fig. 5** Expression analysis of miR-141-3p and miR-200c-3p in Mirc13$^{fl/fl}$ and Mirc13$^{-/-}$
344 mice. Total RNA was isolated from olfactory bulb (OB), frontal cortex (FC), parietal cortex
345 (PC), hippocampus (HP), and cerebellum (CB) of Mirc13$^{fl/fl}$ and Mirc13$^{-/-}$ mice. Basal
346 expression levels of miR-141-3p (**A**) and miR-200c-3p (**B**) were assessed by RT-qPCR

347 using RNA isolated from Mirc13$^{fl/fl}$ mice. (**C**) RNA-FISH was performed to detect
348 expression of miR-141-3p in OB of Mirc13$^{fl/fl}$ and Mirc13$^{-/-}$ mice. Total RNAs isolated from
349 OB (**D** and **I**); FC (**E** and **J**); PC (**F** and **K**); HP (**G** and **L**) and CB (**H** and **M**) were examined
350 for the relative level of miR-141-3p and miR-200c-3p, respectively, by RT-qPCR from
351 Mirc13$^{fl/fl}$ (dark blue column) and Mirc13$^{-/-}$ (red column) mice. Data are presented as mean
352 ± SD (*$p < 0.05$ vs. Mirc13$^{fl/fl}$ control).

353 **DISCUSSION**

354 Generation of the Mirc13^{tm1} line by Park et al. 2012provided the first genetically
355 engineered model for the miR-141/200c cluster(Park, et al. 2012). In their design, a lacZ
356 reporter in association with the En2 splice acceptor and ires sequence, which is similar
357 to the gene trap design(Skarnes, et al. 1992), was aimed to reveal spatial expression of
358 the disrupted endogenous GM15884. Expression of the lacZ reporter is under the
359 transcriptional control of the endogenous GM15884 gene, and with the En2 splice
360 acceptor, lacZ sequence will fuse with exon 1 coding sequence of GM15884. Thus, x-gal
361 staining of the lacZ gene product, β-galactosidase, will faithfully recapitulate the
362 spatiotemporal expression of GM15884(Skarnes, et al. 1992) as well as the miR-
363 141/200c cluster. GM15884 is a lncRNA gene predicted by bioinformatics as described
364 in the Mouse Genome Database(Eppig, et al. 2005)
365 (https://www.informatics.jax.org/marker/key/326668). However, when we performed a
366 blast search of the mouse Expressed Taq Sequence database (dbEST)(Boguski, et al.
367 1993), we were able to identify a mouse cDNA clone, BB612857, of 646 bp. 5' sequence
368 of BB612857 is identical to predicted exon 1 and 2 of GM15884 the rest of the 3'-
369 downstream sequence identical to predicted GM15884 intron 2 sequence. It is well
370 established that EST are derived from transcribed genes (the transcriptome) and dbEST
371 was used to identify transcribed sequences without requiring a fully sequenced

372 genome(Boguski, et al. 1993). Identification of BB612857 confirms the identity of
373 GM15884. This result, together with the tissue-specific lacZ expression, suggests that
374 expression of GM15884/BB612857, as well as Mirc13, is under the control of a tissue-
375 specific Pol II promoter, and our lacZ expression observed in the olfactory bulb and lung
376 in the mice corroborated with the finding of Park et al.

377 Since the Mirc13^{tm1} mouse line was original generated by homologous
378 recombination using ES cells, A β-actin-neo selectable marker was included in the original
379 targeting vector and was retained in the Mirc13^{tm1} mouse line. It has been reported that
380 the Neo cassette with a strong ubiquitous promoter could influence neighboring gene
381 expression(Pham, et al. 1996) and therefore alter phenotype of the mice(Olson, et al.
382 1996; Pan, et al. 2016). Park et al explicitly recommended removal of Neo cassette prior
383 to subsequent use of the mouse line. The Neo cassette together with the lacZ sequence
384 were flanked by FRT sites and could be excised easily by breeding the Mirc13^{tm1} mice
385 with FLP mice. Additional methods by which one could excise the Frt flanked lacZ/Neo
386 cassette is either by electroporation of Flpo mRNA into one-cell embryos(Hashimoto and
387 Takemoto 2015) or infection of one-cell embryos with recombinant adeno-associated
388 viruses expressing Flpo(Nickl, et al. 2024), followed by transferring manipulated embryos
389 into pseudopregnant females for subsequent development. Overall, it is important to
390 generate a functional floxed Mirc13 allele prior to using Cre recombinase for either tissue-
391 specific or global deletion of the miR-141/200c cluster in order to avoid interference from
392 the lacZ/neo elements, including unanticipated knockout of endogenous GM15884 and
393 altering the expression of neighboring genes(McBurney, et al. 2002; Branda and Dymecki
394 2004). Our neighboring gene expression analyses further confirm the influence of
395 presence of β-actin-neo cassette on expression of many neighboring genes such as
396 *ptpn6, phb2* and *atn1* in the Mirc13$^{tm1/tm1}$ mice. The genes *ptpn6, phb2,* and *atn1* each

397 play critical roles in brain function. *Ptpn6* regulates microglial signaling and helps restrain
398 neuroinflammation; its loss can drive excessive immune activation and neuronal
399 injury(He, et al. 2023). *Phb2* maintains mitochondrial integrity and neuronal survival, so
400 deletion can impair energy metabolism and cognitive functions(Xu, et al. 2014). *Atn1* acts
401 as a transcriptional co-regulator in neuronal development and disruption can lead to
402 abnormal differentiation, connectivity, or neurodegeneration(Whitton, et al. 1993). Thus,
403 downregulation of these genes as shown in Mirc13$^{tm1/tm1}$ mice could have significant
404 consequences for neuronal health and brain function. There is no change in expression
405 of these genes in Mirc13$^{fl/fl}$ mice, suggesting that it is essential to remove the lacZ/β-actin-
406 Neo cassettes to obtain fully functional Mirc13 cKO mice for meaningful and precise
407 analyses of their functional roles.

408 Despite the clear breeding plan recommended by Park et al(Park, et al. 2012),
409 several subsequent studies did not adopt the necessary breeding plan. They treated the
410 Mirc13^{tm1} mice, which contain lacZ/β-actin-neo cassettes, as Mirc13 cKO animals and
411 bred them directly with Cre deleters (Guan, et al. 2018; Hoefert, et al. 2018; Ji, et al. 2018;
412 Liu, et al. 2018; Wu, et al. 2019; Xu, et al. 2025). However, Mirc13^{tm1} mice contain three
413 colinear loxP sequences in the same allele (Fig 1A). It is well established that in the
414 presence of Cre, this would lead to different combinations of paired loxP sequences and
415 result in different excisions of loxP flanked sequences. As shown in Fig 6, this could
416 generate three different genotypes dependent on the different pairings of loxP sequences:
417 A). excision of the β-actin-Neo cassette alone; B) excision of Mirc13 alone; and C)
418 excision of β-actin-Neo cassette and Mirc13 together. Nevertheless, in all of these cases,
419 both the endogenous GM15884 and Mirc13 will not express and it is still not possible to
420 decipher the precise functional role of miR-141/200c. Other labs have bred Mirc13^{tm1}
421 pups with β-actin-Flpe mice prior to breeding them with Cre deleters. However, FLPe is

422 not codon-optimized for expression in mammals and the level of FLP protein expression
423 is compromised and excision of the b-actin-neo cassette may not take place in one-cell
424 embryo leading to mosaic animals(Tran, et al. 2017; Mostofa, et al. 2022; Tran, et al.
425 2024). We used Rosa26-FLPo mice, which would overcome the issue of low levels of the
426 FLP gene product(Raymond and Soriano 2007; Wu, et al. 2009; Kranz, et al. 2010). Our
427 breeding plan, as shown in Fig 1, is to remove the lacZ/neo cassettes using ROSA26-
428 FLPo mice, generating a functional Mirc13 floxed allele prior to using Cre mice, such as
429 the germline $Hprt^{CAG\text{-}Cre}$ mice, to achieve global deletion of the Mirc13 allele. These steps
430 ensure that any observed phenotype will be attributed directly to loss of the miR-141/200c
431 cluster, without any confounding contributions from transcriptional silencing or residual
432 neomycin cassette effects.

433 This breeding plan is not merely technical but critical for precise evaluation of the
434 miR-141/200c functional roles. Studies of the miR-200 family—including their roles in late
435 postnatal neurogenesis(Beclin, et al. 2016), stem cell differentiation(Zhang, et al. 2015),
436 and cancer biology(Chen, et al. 2013; Jin, et al. 2017; Tseng, et al. 2017) rely strongly on
437 precise gene dosage and context. Using animals with imprecise genotypes will only
438 hamper validities of the data leading to spurious conclusion and discrepancy among
439 different reports. By adhering to the breeding plan according to the design of the original
440 targeting vector, our work provides a framework to generate unambiguous global and
441 functional conditional knockouts of the miR-141/200c cluster.

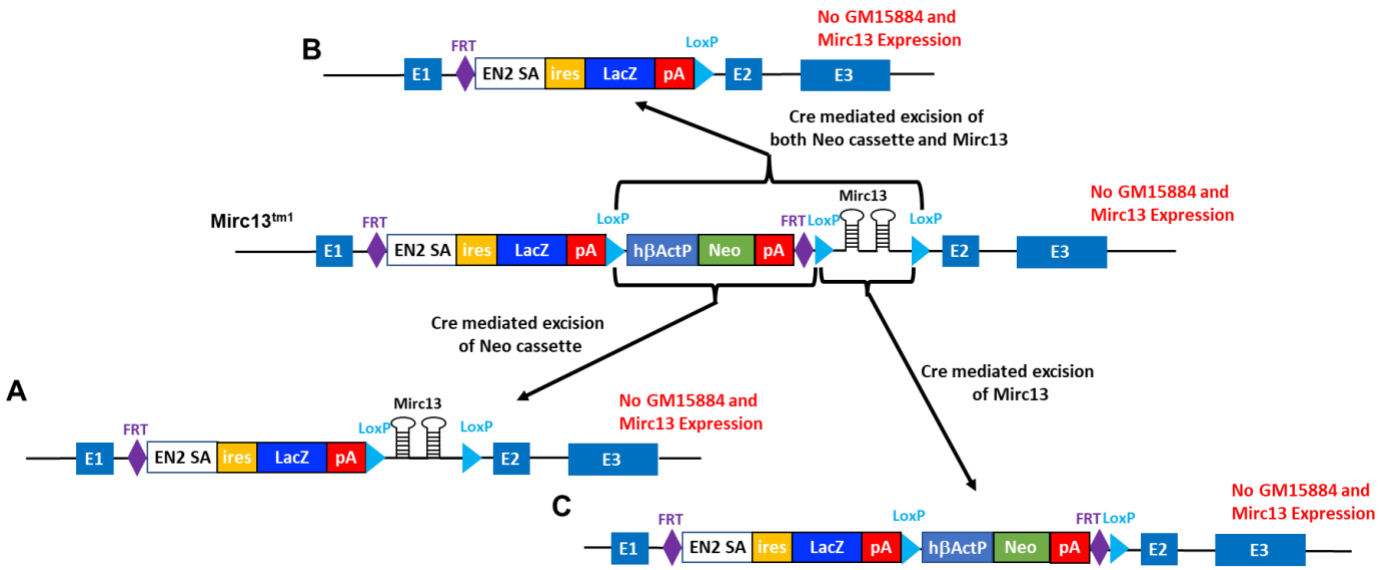

Fig. 6 Breeding Mirc13^{tm1} mice containing three colinear loxP sites with Cre mice could lead to three different genotypes. **A** Excision of the β-actin-Neo cassette; **B** excision of β-actin-Neo cassette together with Mirc13 sequence; and **C** deletion of Mirc13 sequence. In all three different genotypes, both GM15884 and Mirc13 are not expressed due to the presence of the lacZ polyA sequence.

ACKOWLEDGEMENT

Author contributions

RV conceptualized the project. SKY, RS, RV and SPY wrote the manuscript. MKC, RS, SKY and KL performed the experiments. RV and SPY supervised the work. RV secured the funding for the project. All the authors approved the work.

Ethics declarations

Ethical Approval

All experiments were approved and conducted in compliance with the protocols approved (Number: AP-201043-0926) by the Institutional Animal Care and Use Committee (IACUC) at UConn Health. Animal data was reported following the ARRIVE Guidelines.

Declaration of Conflicting Interests

The authors declared no conflicts of interest.

Funding

This work was supported by NIH, United States (1R21NS114981 and R01 NS140176) and REP Convergence (OVPR UConn, United States) grant to R.V.

Data Availability

The data supporting the findings of this study will be available on request from the corresponding author.

482 **REFERENCES**

483 Beclin C, Follert P, Stappers E, Barral S, Coré N, Chevigny A, Magnone V, Lebrigand K,
484 Bissels U, Huylebroeck D, et al. 2016. Corrigendum: miR-200 family controls late steps
485 of postnatal forebrain neurogenesis via Zeb2 inhibition. Sci Rep 6:39368.

486 Bernabeu C, Lopez-Novoa JM, Quintanilla M. 2009. The emerging role of TGF-beta
487 superfamily coreceptors in cancer. Biochim Biophys Acta 1792:954-973.

488 Boguski MS, Lowe TM, Tolstoshev CM. 1993. dbEST--database for "expressed
489 sequence tags". Nat Genet 4:332-333.

490 Branda CS, Dymecki SM. 2004. Talking about a revolution: The impact of site-specific
491 recombinases on genetic analyses in mice. Dev Cell 6:7-28.

492 Chen D, Zhang Y, Wang J, Chen J, Yang C, Cai K, Wang X, Shi F, Dou J. 2013.
493 MicroRNA-200c overexpression inhibits tumorigenicity and metastasis of CD117+CD44+
494 ovarian cancer stem cells by regulating epithelial-mesenchymal transition. J Ovarian Res
495 6:50.

496 Choi PS, Zakhary L, Choi WY, Caron S, Alvarez-Saavedra E, Miska EA, McManus M,
497 Harfe B, Giraldez AJ, Horvitz HR, et al. 2008. Members of the miRNA-200 family regulate
498 olfactory neurogenesis. Neuron 57:41-55.

499 Clausen BE, Burkhardt C, Reith W, Renkawitz R, Förster I. 1999. Conditional gene
500 targeting in macrophages and granulocytes using LysMcre mice. Transgenic Res 8:265-
501 277.

502 Eppig JT, Bult CJ, Kadin JA, Richardson JE, Blake JA, Anagnostopoulos A, Baldarelli
503 RM, Baya M, Beal JS, Bello SM, et al. 2005. The Mouse Genome Database (MGD): from
504 genes to mice--a community resource for mouse biology. Nucleic Acids Res 33:D471-
505 475.

506 Guan T, Dominguez CX, Amezquita RA, Laidlaw BJ, Cheng J, Henao-Mejia J, Williams
507 A, Flavell RA, Lu J, Kaech SM. 2018. ZEB1, ZEB2, and the miR-200 family form a
508 counterregulatory network to regulate CD8(+) T cell fates. J Exp Med 215:1153-1168.

509 Hashimoto M, Takemoto T. 2015. Electroporation enables the efficient mRNA delivery
510 into the mouse zygotes and facilitates CRISPR/Cas9-based genome editing. Sci Rep
511 5:11315.

512 He Y, Nan D, Wang H. 2023. Role of Non-Receptor-Type Tyrosine Phosphatases in
513 Brain-Related Diseases. Mol Neurobiol 60:6530-6541.

514 Hoefert JE, Bjerke GA, Wang D, Yi R. 2018. The microRNA-200 family coordinately
515 regulates cell adhesion and proliferation in hair morphogenesis. J Cell Biol 217:2185-
516 2204.

517 Humphries B, Yang C. 2015. The microRNA-200 family: small molecules with novel roles
518 in cancer development, progression and therapy. Oncotarget 6:6472-6498.

519 Isgrò MA, Bottoni P, Scatena R. 2015. Neuron-Specific Enolase as a Biomarker:
520 Biochemical and Clinical Aspects. Adv Exp Med Biol 867:125-143.

521 Janssen HL, Reesink HW, Lawitz EJ, Zeuzem S, Rodriguez-Torres M, Patel K, van der
522 Meer AJ, Patick AK, Chen A, Zhou Y, et al. 2013. Treatment of HCV infection by targeting
523 microRNA. N Engl J Med 368:1685-1694.

524 Ji ML, Jiang H, Zhang XJ, Shi PL, Li C, Wu H, Wu XT, Wang YT, Wang C, Lu J. 2018.
525 Preclinical development of a microRNA-based therapy for intervertebral disc
526 degeneration. Nat Commun 9:5051.

527 Jin T, Suk Kim H, Ki Choi S, Hye Hwang E, Woo J, Suk Ryu H, Kim K, Moon A, Kyung
528 Moon W. 2017. microRNA-200c/141 upregulates SerpinB2 to promote breast cancer cell
529 metastasis and reduce patient survival. Oncotarget 8:32769-32782.

530 Kranz A, Fu J, Duerschke K, Weidlich S, Naumann R, Stewart AF, Anastassiadis K. 2010.
531 An improved Flp deleter mouse in C57Bl/6 based on Flpo recombinase. Genesis 48:512-
532 520.

533 Lee RC, Feinbaum RL, Ambros V. 1993. The C. elegans heterochronic gene lin-4
534 encodes small RNAs with antisense complementarity to lin-14. Cell 75:843-854.

535 Liu B, Du R, Zhou L, Xu J, Chen S, Chen J, Yang X, Liu DX, Shao ZM, Zhang L, et al.
536 2018. miR-200c/141 Regulates Breast Cancer Stem Cell Heterogeneity via Targeting
537 HIPK1/β-Catenin Axis. Theranostics 8:5801-5813.

538 McBurney MW, Mai T, Yang X, Jardine K. 2002. Evidence for repeat-induced gene
539 silencing in cultured Mammalian cells: inactivation of tandem repeats of transfected
540 genes. Exp Cell Res 274:1-8.

541 Mostofa MG, Tran M, Gilling S, Lee G, Fraher O, Jin L, Kang H, Park YK, Lee JY, Wang
542 L, et al. 2022. MicroRNA-200c coordinates HNF1 homeobox B and apolipoprotein O
543 functions to modulate lipid homeostasis in alcoholic fatty liver disease. J Biol Chem
544 298:101966.

545 Nickl P, Jenickova I, Elias J, Kasparek P, Barinka C, Kopkanova J, Sedlacek R. 2024.
546 Multistep allelic conversion in mouse pre-implantation embryos by AAV vectors. Sci Rep
547 14:20160.

548 Olson EN, Arnold HH, Rigby PW, Wold BJ. 1996. Know your neighbors: three phenotypes
549 in null mutants of the myogenic bHLH gene MRF4. Cell 85:1-4.

550 Pan Y, Zhang L, Liu Q, Li Y, Guo H, Peng Y, Peng H, Tang B, Hu Z, Zhao J, et al. 2016.
551 Insertion of a knockout-first cassette in Ampd1 gene leads to neonatal death by disruption
552 of neighboring genes expression. Sci Rep 6:35970.

553 Park CY, Jeker LT, Carver-Moore K, Oh A, Liu HJ, Cameron R, Richards H, Li Z, Adler
554 D, Yoshinaga Y, et al. 2012. A resource for the conditional ablation of microRNAs in the
555 mouse. Cell Rep 1:385-391.

556 Pasquinelli AE, Reinhart BJ, Slack F, Martindale MQ, Kuroda MI, Maller B, Hayward DC,
557 Ball EE, Degnan B, Müller P, et al. 2000. Conservation of the sequence and temporal
558 expression of let-7 heterochronic regulatory RNA. Nature 408:86-89.

559 Pham CT, MacIvor DM, Hug BA, Heusel JW, Ley TJ. 1996. Long-range disruption of gene
560 expression by a selectable marker cassette. Proc Natl Acad Sci U S A 93:13090-13095.

561 Raja R, Dumontier E, Phen A, Cloutier JF. 2024. Insertion of a neomycin selection
562 cassette in the Amigo1 locus alters gene expression in the olfactory epithelium leading to
563 region-specific defects in olfactory receptor neuron development. Genesis 62:e23594.

564 Raymond CS, Soriano P. 2007. High-efficiency FLP and PhiC31 site-specific
565 recombination in mammalian cells. PLoS One 2:e162.

566 Rishik S, Hirsch P, Grandke F, Fehlmann T, Keller A. 2025. miRNATissueAtlas 2025: an
567 update to the uniformly processed and annotated human and mouse non-coding RNA
568 tissue atlas. Nucleic Acids Res 53:D129-d137.

569 Skarnes WC, Auerbach BA, Joyner AL. 1992. A gene trap approach in mouse embryonic
570 stem cells: the lacZ reported is activated by splicing, reflects endogenous gene
571 expression, and is mutagenic in mice. Genes Dev 6:903-918.

572 Skarnes WC, Rosen B, West AP, Koutsourakis M, Bushell W, Iyer V, Mujica AO, Thomas
573 M, Harrow J, Cox T, et al. 2011. A conditional knockout resource for the genome-wide
574 study of mouse gene function. Nature 474:337-342.

575 Small EM, Frost RJ, Olson EN. 2010. MicroRNAs add a new dimension to cardiovascular
576 disease. Circulation 121:1022-1032.

577 Tang SH, Silva FJ, Tsark WM, Mann JR. 2002. A Cre/loxP-deleter transgenic line in
578 mouse strain 129S1/SvImJ. Genesis 32:199-202.

579 Testa G, Schaft J, van der Hoeven F, Glaser S, Anastassiadis K, Zhang Y, Hermann T,
580 Stremmel W, Stewart AF. 2004. A reliable lacZ expression reporter cassette for
581 multipurpose, knockout-first alleles. Genesis 38:151-158.

582 Tran M, Gilling S, Wu J, Wang L, Shin DJ. 2024. miR-141/200c contributes to ethanol-
583 mediated hepatic glycogen metabolism. Mol Metab 84:101942.

584 Tran M, Lee SM, Shin DJ, Wang L. 2017. Loss of miR-141/200c ameliorates hepatic
585 steatosis and inflammation by reprogramming multiple signaling pathways in NASH. JCI
586 Insight 2.

587 Tseng JH, Bisogna M, Hoang LN, Olvera N, Rodriguez-Aguayo C, Lopez-Berestein G,
588 Sood AK, Levine DA, Jelinic P. 2017. miR-200c-driven Mesenchymal-To-Epithelial
589 Transition is a Therapeutic Target in Uterine Carcinosarcomas. Sci Rep 7:3614.

590 van Rooij E, Kauppinen S. 2014. Development of microRNA therapeutics is coming of
591 age. EMBO Mol Med 6:851-864.

592 Verma R, Ritzel RM, Harris NM, Lee J, Kim T, Pandi G, Vemuganti R, McCullough LD.
593 2018. Inhibition of miR-141-3p Ameliorates the Negative Effects of Poststroke Social
594 Isolation in Aged Mice. Stroke 49:1701-1707.

595 Whitton C, Palmer E, Alkuraya F. 1993. ATN1-Related Neurodevelopmental Disorder. In:
596 Adam MP, Bick S, Mirzaa GM, Pagon RA, Wallace SE, Amemiya A, editors.
597 GeneReviews(®). Seattle (WA): University of Washington, Seattle

598 Copyright © 1993-2026, University of Washington, Seattle. GeneReviews is a registered
599 trademark of the University of Washington, Seattle. All rights reserved.

600 Wightman B, Ha I, Ruvkun G. 1993. Posttranscriptional regulation of the heterochronic
601 gene lin-14 by lin-4 mediates temporal pattern formation in C. elegans. Cell 75:855-862.

602 Wu MJ, Chen YS, Kim MR, Chang CC, Gampala S, Zhang Y, Wang Y, Chang CY, Yang
603 JY, Chang CJ. 2019. Epithelial-Mesenchymal Transition Directs Stem Cell Polarity via
604 Regulation of Mitofusin. Cell Metab 29:993-1002.e1006.

605 Wu Q, Ye X, Xiong Y, Zhu H, Miao J, Zhang W, Wan J. 2016. The Protective Role of
606 microRNA-200c in Alzheimer's Disease Pathologies Is Induced by Beta Amyloid-
607 Triggered Endoplasmic Reticulum Stress. Front Mol Neurosci 9:140.

608 Wu Y, Wang C, Sun H, LeRoith D, Yakar S. 2009. High-efficient FLPo deleter mice in
609 C57BL/6J background. PLoS One 4:e8054.

610 Xu L, Griffiths B, Sun X, Greer M, Chang H, McMillin E, Manis E, Russo I, Dean CAJ,
611 Stary CM. 2025. Conditional neuronal deletion of microRNA-141/200c cluster, but not
612 microRNA-181a/b-1 cluster, is protective against experimental stroke in male mice.
613 Physiol Rep 13:e70505.

614 Xu T, Fan X, Tan Y, Yue Y, Chen W, Gu X. 2014. Expression of PHB2 in rat brain cortex
615 following traumatic brain injury. Int J Mol Sci 15:3299-3318.

616 Yadav SK, Dhuri K, Gamiotea-Turro D, Cormier MK, Patel V, Yadawa AK, Pathuri M,
617 Bahal R, Verma R. 2024. Exploring the therapeutic potential of syPNA-141:
618 Pharmacodynamics and mechanistic insights during ischemic stroke recovery. Mol Ther
619 Nucleic Acids 35:102355.

620 Zhang J, Gao Y, Yu M, Wu H, Ai Z, Wu Y, Liu H, Du J, Guo Z, Zhang Y. 2015. Retinoic
621 Acid Induces Embryonic Stem Cell Differentiation by Altering Both Encoding RNA and
622 microRNA Expression. PLoS One 10:e0132566.

623